ORIGINAL ARTICLE

Association of inflammation of the left anterior descending coronary artery with cardiovascular risk factors, plaque burden and pericardial fat volume: a PET/CT study

Tobias Saam · Axel Rominger · Sarah Wolpers · Konstantin Nikolaou · Carsten Rist ·
Martin Greif · Paul Cumming · Alexander Becker · Stefan Foerster ·
Maximilian F. Reiser · Peter Bartenstein · Marcus Hacker

Abstract
Purpose Measurements of [18F]fluorodeoxyglucose (FDG) uptake as a potential marker of the inflammatory activity of the vessel wall could be useful to identify vulnerable atherosclerotic plaques. The purpose of this study was to correlate the FDG uptake in the left anterior descending coronary artery (LAD) with cardiovascular risk factors, pericardial fat volume (PFV) and calcified plaque burden (CPB).
Methods A total of 292 consecutive tumour patients were examined by whole-body FDG PET and contrast-enhanced CT. The blood pool-corrected standardized uptake value (target to background ratio, TBR) was measured in the LAD, and the contrast-enhanced CT images were used to measure the PFV and the CPB. The Spearman correlation coefficient and the unpaired t test were used for statistical comparison between image-based results and cardiovascular risk factors.
Results Vascular FDG uptake could be measured for 161 of 292 (55%) patients without myocardial uptake, but the vessel uptake could not be distinguished in the other patients, due to pervasive myocardial uptake. The TBR of the LAD showed significant correlations with hypertension ($R=0.18$; $p<0.05$), coronary heart disease ($R=0.19$; $p<0.05$), body mass index (BMI) ($R=0.19$; $p<0.05$), CPB ($R=0.36$; $p<0.001$) and PFV ($R=0.20$; $p<0.05$), but not with other risk factors. Patients with a TBR in the upper tertile had a larger CPB and a higher PFV than patients with a TBR in the lower tertile (9.1 vs 3.5; $p<0.001$ for CPB and 92.2 vs 71.5 mm³; $p<0.05$ for PVF).
Conclusion FDG uptake measurement in the LAD correlates with hypertension, coronary heart disease, BMI, PFV and CPB. However, due to myocardial FDG uptake these measurements are only feasible in one half of the patients.

Keywords Atherosclerosis · Plaque imaging · FDG · PET/CT · Inflammation · Coronary arteries

Tobias Saam and Axel Rominger contributed equally to this work.

T. Saam · K. Nikolaou · C. Rist · M. F. Reiser
Institute of Clinical Radiology, University of Munich,
Munich, Germany

A. Rominger · S. Wolpers · P. Cumming · S. Foerster ·
P. Bartenstein · M. Hacker (✉)
Department of Nuclear Medicine, University of Munich,
Marchioninistr. 15,
81377 Munich, Germany
e-mail: marcus.hacker@med.uni-muenchen.de

M. Greif · A. Becker
Department of Cardiology, University of Munich,
Munich, Germany

Introduction

Atherosclerosis is one of the leading causes of morbidity and mortality in the developed world [1]. Indeed, atherosclerotic disease accounts for approximately 25% of ischaemic strokes and for the majority of myocardial infarctions and sudden cardiac deaths [2, 3]. Despite major advances in its treatment, a substantial percentage of seemingly healthy atherosclerosis patients die without prior symptoms [3]. New imaging methods promise to facilitate screening of high-risk patients and identify those with vascular lesions that are vulnerable to thrombosis, the so-called vulnerable plaques, making timely intervention possible.

In 2003 a group of researchers in the field of atherosclerosis, including pathologists, clinicians, molecu-

lar biologists and imaging scientists, published two consensus documents in which they defined the key features of vulnerable plaques [2, 3]. It was determined that the presence of active inflammation is characteristic of the vulnerable plaque. Indeed, inflammation plays a critical role in plaque initiation, progression and disruption and represents an emerging target in the treatment of atherosclerosis. Systemic indicators of inflammation, such as C-reactive protein and interleukin-6, can easily be obtained by testing blood samples, and it has been shown that elevated levels of several inflammatory markers in circulation are predictive of coronary artery disease [4]. However, these markers should not be considered as causative factors, but rather as indicators of the disease process at inflammatory sites [4]. It is precisely this local inflammatory process that can be revealed by non-invasive imaging methods targeting the vulnerable plaque [3, 5].

Recent studies have suggested that whole-body positron emission tomography (PET) with [18F]fluorodeoxyglucose (FDG) is a reliable and promising technique to image and quantify plaque inflammation [6, 7]. Recent PET/computed tomography (CT) studies have shown a good correlation between carotid plaque FDG uptake in vivo and the intensity of macrophage staining in the corresponding histological sections [8], suggesting that FGD PET can serve as a biomarker of vessel wall inflammation. Several recent studies have shown weak, but highly significant correlations between FDG uptake in atherosclerotic plaques and cardiovascular risk factors [9–11]. Furthermore, it has been shown that FDG uptake is higher in symptomatic carotid plaques compared to asymptomatic plaques of the same patient [7]. Another recent study has shown an association between FDG uptake in atherosclerotic plaques and the occurrence of future cardio- or cerebrovascular events [11]. Thus, whole-body FDG PET/CT is emerging as a promising tool for non-invasive assessment of the extent of inflammatory activity in patients with atherosclerotic disease. To date, most of this work has focussed on relatively large arteries, such as the aorta or the carotid arteries. While pathological features in these arteries are likely representative of a general atherosclerotic disease, most of the deaths result from thromboembolic complications of inflammatory plaques specifically in the coronary arteries [12]. Interestingly, the majority of these cardiovascular events occur in coronary arteries with <50% stenosis [13], indicating that information about luminal stenosis is insufficient to predict a plaque's vulnerability. Several other imaging methods, such as intravascular ultrasound (IVUS) [14] and coronary CT [15], have been proposed for assessing coronary atherosclerotic plaques. Although the IVUS and CT methods are both sufficient to quantify the atherosclerotic plaque burden, and coronary CT can differentiate between soft and hard plaques [15], neither of these imaging modalities are informative about the inflammatory activity in coronary plaques.

The combination of PET and CT in a single apparatus enables the exact anatomical assignment of focally increased FDG uptake to specific arterial vessel segments, such as the coronary arteries. Furthermore, the CT modality allows the detection and quantification of the calcified plaque burden (CPB) and the quantification of the pericardial fat volume (PFV). It is well documented that calcified coronary atherosclerotic plaque burden is an independent risk factor for future cardiovascular events [16], and several recent publications [17, 18] have suggested a potential role for PFV as a biomarker for atherosclerosis. In the present study we tested the hypothesis that FDG uptake measured in the left anterior descending coronary artery (LAD) of tumour patients correlates with CT-based imaging markers of atherosclerosis, i.e. PFV and CPB, and with other cardiovascular risk factors.

Materials and methods

Patients

We recruited 292 consecutive patients who had been referred for a contrast-enhanced PET/CT scan at our institution due to a non-cardiovascular indication, i.e. oncology. Patients with prior or ongoing steroid medication, inflammation of unknown origin, sepsis or vasculitis were excluded from our study. Age, body mass index (BMI) and common cardiovascular risk factors, such as hypertension, smoking, family history of cardio- or cerebrovascular disease, diabetes and presence of coronary heart disease were recorded. The study protocol was approved by the local Clinical Institutional Review Board and complied with the Declaration of Helsinki.

Imaging technique

All patients underwent FDG PET/CT on a Philips Gemini PET/CT scanner (Philips Medical Systems, Hamburg, Germany), consisting of a gadolinium samarium oxalate (GSO) full-ring PET scanner and a CT with two detector rows. Prior to scanning, the patients fasted for at least 6 h to ensure a serum glucose level below 130 mg/ml. Patients received 20 mg furosemide and 20 mg butylscopolamine bromide and 210–420 MBq FDG (= 5 MBq/kg body weight) in a single intravenous bolus injection. The patients rested for 45 min in a comfortable position in a quiet room and were then conveyed to the scanning suite. At least

60 min and not more than 90 min after FDG administration, transmission data were acquired via a low-dose CT scan (20 mAs, 140 kV, 512×512 matrix, 6 mm slice thickness, 5 mm/s increment, 0.5 s rotation time, 1.5 pitch index) extending from the base of the skull to the proximal thighs. Subsequently, a contrast-enhanced CT scan (Ultravist 370, 370 mg iodine/ml, Bayer-Schering AG, Berlin, Germany) was performed with a slice thickness of 3 mm (195 mAs, 120 kV, 512×512 matrix, 5 mm/s increment, 0.5 s rotation time, 1.5 pitch index). The delay between contrast injection and CT scan was 70 s. Three-dimensional (3-D) PET emission scans were subsequently acquired in the caudocranial direction with a 144×144 matrix. After scatter and decay correction, the PET data were reconstructed iteratively with and without attenuation correction and then reoriented in the axial, sagittal and coronal planes. To obtain the 3-D reconstruction, we used an algorithm based on the row action maximum likelihood algorithm, implemented with the PET-View software (Philips Medical Systems, Hamburg, Germany).

Image analysis

FDG uptake

PET/CT scans were read by an experienced reader (M.H.), who was blind to patient information and clinical information relevant to cardiovascular disease. Patients with significant FDG uptake in any domain of the myocardium were excluded from further analysis. The position of the LAD was identified on the contrast-enhanced CT images (see Fig. 1a, b). Fused PET/CT images, which were manually corrected in the case of a general misalignment of the large organs/vessels or surface contours, were used for multiple region of interest (ROI) analysis of the LAD. Maximal standardized uptake values (SUV_{max}) were measured according to a previously described method [19]. Briefly, from the left sinus of Valsalva to the outlet of the first diagonal branch of the LAD, which we herein define as LAD, we manually placed ordinary circular ROIs of fixed size in all patients. The size was chosen in order to assure that the whole vessel circumference was measured in each individual patient. Finally, correct placement of the ROI within the lumen of the coronary artery was visually verified in each case by inspection in all three planes of the fused PET/CT images, using the zoom display tool and moving them along the long axis to find the regions of SUV_{max}.

For blood pool SUV measurements, three different ROIs were placed in both the mid-lumen of the inferior and superior vena cavae with a fixed diameter of 1 cm, as previously described [11, 19]; the mean of the six measurements was defined as the $SUV_{blood\ pool}$ (Fig. 2). The quotient of SUV_{max} and $SUV_{blood\ pool}$ was designated as the target to background ratio (TBR) for the LAD.

Plaque burden

The CT scans were examined for the presence of calcified plaque (CP) in the walls of the right and left common carotid artery, ascending aorta, aortic arch, descending aorta, abdominal aorta and both iliac arteries. A cut-off value of 130 HU was used for the identification of calcification. The amount of calcification was semi-quantitatively determined according to the following scale [11]: A score of "0" was assigned when CPs were absent, "1" was assigned when a single, small CP was found, encompassing less than 10% of the vessel circumference, a score of "2" was assigned if the CP involved 10–25% of the vessel circumference, "3" if 25–50% and "4" if >50% of the vessel circumference was involved (see Fig. 1c). The total CPB was calculated as the sum of the CP values in the eight vessels listed above.

Pericardial fat

The PFV (cm^3) was measured using the volume analysis software tool of our cardiac workstation Leonardo (Siemens Healthcare, Erlangen, Germany). We defined pericardial fat as the composite of epicardial fat and paracardial fat, as identified by HU ranging from −30 to −200 [18, 20].

Reproducibility

To assess intra- and inter-reader reproducibility, TBR_{LAD}, CP and PFV measurements were repeated in 20 patients 8 weeks after the initial review by the same reviewer (M. H.) and by a second reviewer (K.N.).

Statistical analysis

Categoric variables are presented as absolute and relative frequencies, while continuous variables are presented as mean and standard deviation. Patients were grouped into tertiles based on their TBR_{LAD} values. For between-group comparisons for the TBR tertiles and the comparison between the patients with and without myocardial FDG uptake, unpaired Student's t tests were used for parametric data, and Mann-Whitney U rank sum tests were used for non-parametric data. The Spearman correlation coefficients were calculated for the relationships between the three image-based end-points (TBR_{LAD}, CPB and PFV) and age, BMI and the occurrence of
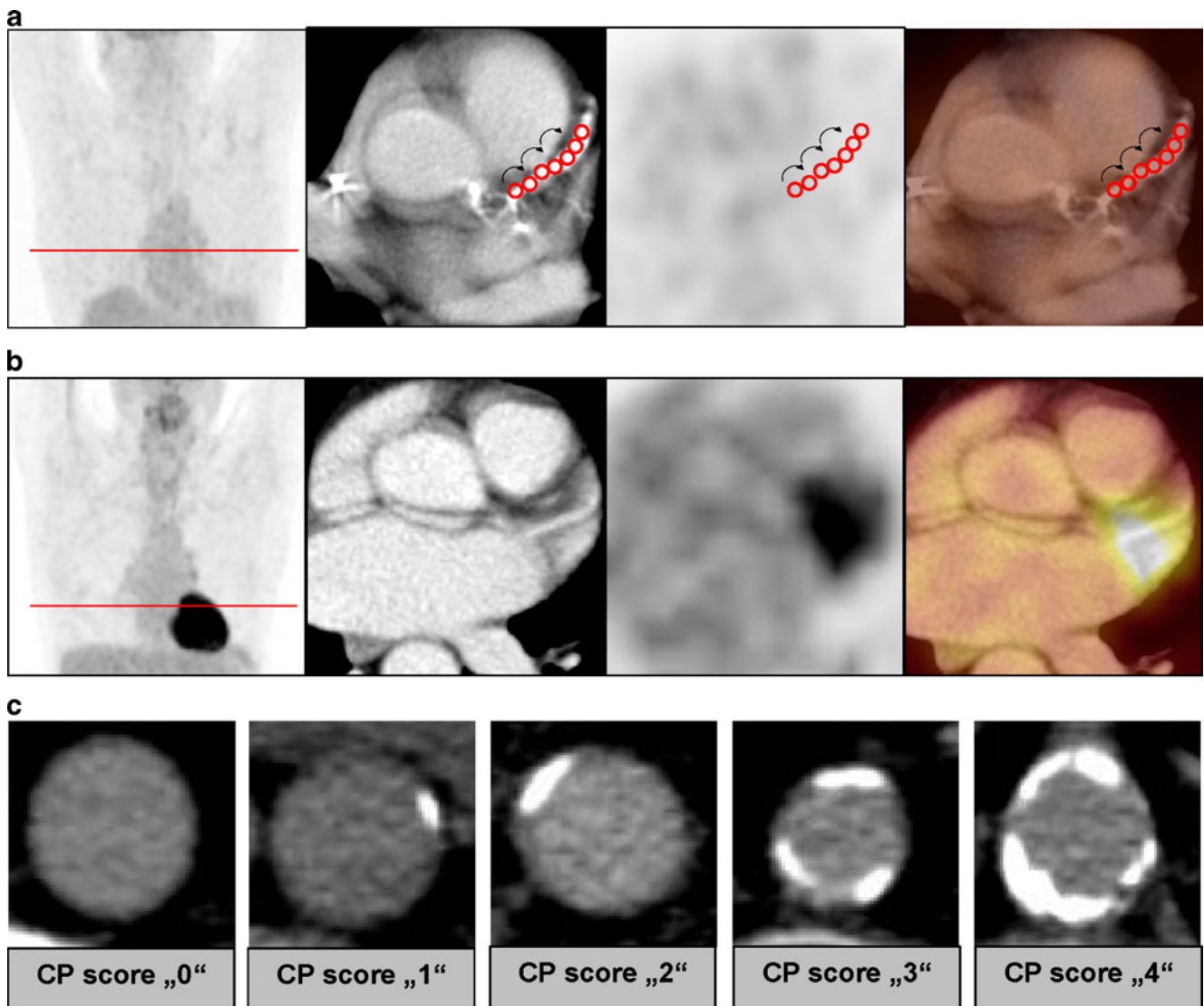
Fig. 1 PET/CT image analysis. **a** Example of the SUV measurement in the left coronary artery. The *red circles* indicate ROIs of the same size, which are slid along the course of the vessel, indicated with *black arrows*. Within the ROIs the SUV and subsequently the TBR was calculated. Coronal PET image on the *left* shows no discernible FDG uptake in the myocardium. Axial CT images were used to localize the left coronary artery, and measurements of the SUV were then performed on the fused PET/CT images along the course of the left coronary artery. The SUV_{max} in this patient was 0.9 and the mean venous SUV was 1.0, resulting in a target to blood pool ratio of 0.9 (low tertile). **b** PET/CT images of a 77-year-old female patient with a history of hypercholesterolaemia and hypertension. Coronal PET image on the *left* shows a homogeneous FDG uptake in the myocardium, which hampers the measurements of the SUV. FDG uptake on the axial PET images is caused by the myocardium and not by the left coronary artery. Patients with myocardial FDG uptake were excluded from further analysis. **c** Examples of the calcified plaque (CP) scoring system [9]. Images from *left to right*, score of "0", no calcified plaque; score of "1", CP covered less than 10% of the vessel circumference; score of "2", CP involved 10–25% of the vessel circumference; score of "3", 25–50% of the vessel circumference; and score of "4", more than 50% of the vessel circumference involved

cardiovascular risk factors. Multiple linear regression analysis was used to accommodate for differences in risk factors, age and BMI.

Intra-class correlation coefficients (ICCs) with 95% confidence intervals (CI) were calculated to test the intra- and inter-reader agreement for the TBR_{LAD} and CPB scores. Here, an ICC value of unity indicates perfect agreement, and ICC values greater than 0.8 are generally accepted as a measure of excellent reproducibility [21].

Results

Patient population

FDG uptake measurements in the LAD proved to be feasible in 161 of 292 (55.1%) patients. In all other patients, the presence of substantial myocardial FDG uptake interfered with the measurement of FDG uptake in the LAD. These 131 patients were excluded from further
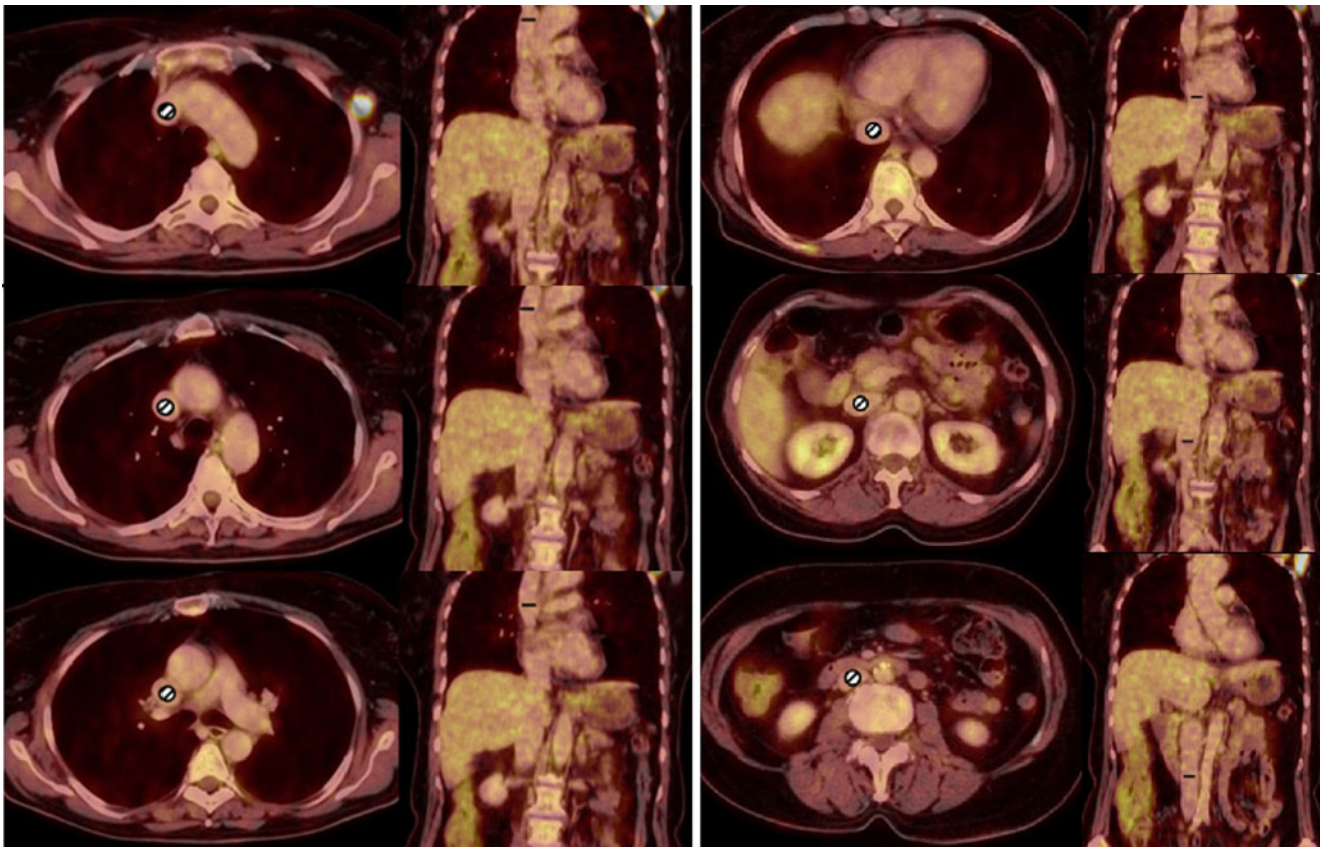
Fig. 2 Determination of the $SUV_{blood\ pool}$. Three ROIs were placed within the lumen of the superior vena cava (*left*) as well as the inferior vena cava (*right*) using fused axial PET/CT images. The slice position is indicated on the corresponding coronal slices. The mean of the six measurements was defined as the $SUV_{blood\ pool}$

statistical analysis. No significant differences were found between patients with and without myocardial FDG uptake for age, gender, BMI and all cardiovascular risk factors (data not shown). Relevant baseline characteristics of the patients included are reported in Table 1.

Correlation of baseline parameters

Table 2 shows the correlations of the image-based parameters (TBR in the LAD, CPB and PFV) with the baseline clinical characteristics. Within the group, there were weak but significant correlations between TBR and hypertension ($R=0.18$; $p<0.05$), coronary heart disease ($R=0.19$; $p<0.05$), BMI ($R=0.19$; $p<0.05$), PFV ($R=0.20$; $p<0.05$) and CPB ($R=0.36$; $p<0.001$). When multiple regression analysis was performed to accommodate for differences in age, BMI and risk factors, correlations between TBR and BMI and CPB remained significant ($p=0.02$ for BMI and $p<0.001$ for CPB). CPB showed highly significant correlations with age ($R=0.57$; $p<0.01$), male gender ($R=0.22$; $p<0.01$), PFV ($R=0.40$; $p<0.01$) and all cardiovascular risk factors except hypercholesterolaemia ($R=0.18-0.33$; $p<0.05$). When multiple regression analysis was performed to

Table 1 Baseline characteristics of the study cohort ($n=161$)

Parameters	
Age (years)	58.9±12.5 (17–85)
Men	64 (39.7)
BMI	25.4±4.8 (16.0–48.0)
Cardiovascular risk factors	
Hypercholesterolaemia	35 (21.7)
Hypertension	38 (23.6)
Active smoker	21 (13.0)
Diabetes mellitus	9 (5.6)
Family history of CVD	40 (24.8)
Coronary heart disease	20 (12.4)
CPB	5.9±6.3 (0–30)
PFV	81.7±47.1 (14–256)
TBR_{LAD}	1.3±0.4 (0.99–1.98)

Values are mean ± standard deviation (range or percentage)

CVD cardiovascular disease, *CPB* calcified plaque burden, *PFV* pericardial fat volume, TBR_{LAD} target to blood pool ratio of the left coronary artery

Table 2 Baseline characteristics of the study cohort ($n=161$) in correlation with TBR_{LAD}, CPB and PFV

	TBR_{LAD}	CPB	PFV
Age	0.18*	0.57**	0.41**
Male gender	n.s.	0.22**	0.46**
BMI	0.19*	n.s.	0.50**
Coronary heart disease	0.19*	0.22**	n.s.
Hypertension	0.18*	0.18*	0.22**
Smoking	n.s.	0.23*	n.s.
Diabetes	n.s.	0.22**	0.24**
Hypercholesterolaemia	n.s.	n.s.	0.19*
TBR_{LAD}	–	0.36**	0.20**
CPB	0.36**	–	0.40**
PFV	0.20**	0.40**	–

TBR_{LAD} target to blood pool ratio of the left coronary artery, *CPB* calcified plaque burden, *PFV* pericardial fat volume

Spearman correlation coefficients: *$p<0.05$; **$p<0.01$

accommodate for differences in age, BMI and risk factors, correlations between CPB and age ($p<0.001$), TBR ($p<0.01$), smoking ($p<0.01$), diabetes ($p<0.05$) and coronary heart disease ($p<0.05$) remained significant. PFV showed moderate and highly significant correlations with age ($R=0.41$; $p<0.01$), male gender ($R=0.46$; $p<0.01$) and BMI ($R=0.50$; $p<0.01$) and weak correlations with hypertension, diabetes and hypercholesterolaemia ($R=0.19–0.31$; $p<0.05$). When multiple regression analysis was performed to accommodate for differences in age, BMI and risk factors, correlations between PFV and BMI ($p<0.001$), age ($p<0.001$), smoking ($p=0.005$) and CPB ($p<0.05$) remained significant.

Tertile-based analysis

Patients were grouped into tertiles according to their TBR score in the LAD. The TBR scores ranged from 0.42 to 1.21 in the low tertile, 1.22 to 1.43 in the middle tertile and 1.44 to 2.42 in the high tertile. Figure 3 shows PFV, CPB, BMI, age and the prevalence of cardiovascular risk factors according to these TBR tertiles. Patients within the high TBR tertile had larger CPB, higher PFV, were older and had a higher prevalence of hypertension and coronary heart disease than did patients in the low TBR tertile (9.1 vs 3.5, $p<0.001$ for CPB; 92.2 vs 71.5 mm^3, $p<0.05$ for PFV; 62.6 vs 57.2, $p<0.05$ for age; 35.2 vs 16.7%, $p<0.05$ for hypertension; and 20.4 vs 5.6%, $p<0.05$ for coronary heart disease). Furthermore, patients within the high TBR tertile had a larger CPB and were older as compared to patients within the middle TBR tertile (9.1 vs 5.1; $p=0.001$ for CPB and 62.6 vs 56.9, $p<0.05$ for age). PET and CT images

from representative patients within the low (Fig. 4) and high (Fig. 5) TBR tertiles are illustrated.

Reproducibility

Intra-reader ICC was 0.97 (95% CI: 0.93–0.99) for TBR, 0.99 (95% CI: 0.96–0.99) for CPB and 0.98 (95% CI: 0.93–1.00) for PFV. Inter-reader ICC was 0.98 (95% CI: 0.94–0.99) for CPB, 0.82 (95% CI: 0.59–0.93) for TBR and 0.94 (95% CI: 0.88–99) for PFV.

Discussion

Findings of this cross-sectional study showed highly significant correlations between FDG uptake in the wall of the left coronary artery and the score for the calcified atherosclerotic plaque burden, the PFV and cardiovascular risk factors in patients who were investigated for non-cardiovascular indications. Furthermore, the patients falling within the high tertile for TBR in the LAD had higher CPB and PFV scores, were older and had a higher prevalence of hypertension and coronary heart disease than did the patients in the low tertile for TBR. These significant correlations indicate TBR measurements of the LAD to be a useful tool for assessing the local inflammatory process of atherosclerotic disease. The present findings thus elaborate upon earlier reports of significant correlations between arterial FDG uptake and the presence of conventional cardiovascular risk factors as well as arterial wall calcifications in large peripheral arteries [9–11, 22, 23]. Indeed, it has been recently shown [11] that increased FDG uptake in the aorta, carotid and iliac arteries is significantly associated with the occurrence of cardio- or cerebrovascular events during follow-up in oncological patients without cardiac symptoms or history of coronary heart disease.

To date there have been few imaging studies of inflammatory activity in the coronary arteries. FDG uptake measurements in these vessels are degraded by heart motion and respiration, which impair the image quality of both FDG PET and CT, and make it difficult to correctly allocate regions with FDG accumulation to specific coronary lesions. In the present study, 2-slice CT scans were used to guide the FDG measurements, and TBR quantification was sufficient at least in the proximal portion of the left coronary artery. A recent study by Wykrzykowska et al. [24] showed that allocation of FDG uptake to specific coronary lesions was feasible with a non-cardiac 4-slice PET/CT scanner. They reported a nearly significant correlation ($p=0.07$) between the FDG signal in coronary vessels and the presence of angiographic disease in 32 oncological patients.

Fig. 3 Cardiovascular risk factors and PET/CT variables according to TBR_{LAD} tertiles. To enable a better graphic visualization CPB was multiplied by a factor of 10. The unpaired Student's *t* test was used for statistical comparison. *CHD* coronary heart disease, *FH* family history of cardio- or cerebrovascular disease, *PFV* pericardial fat volume, *CPB* calcified plaque burden, *BMI* body mass index
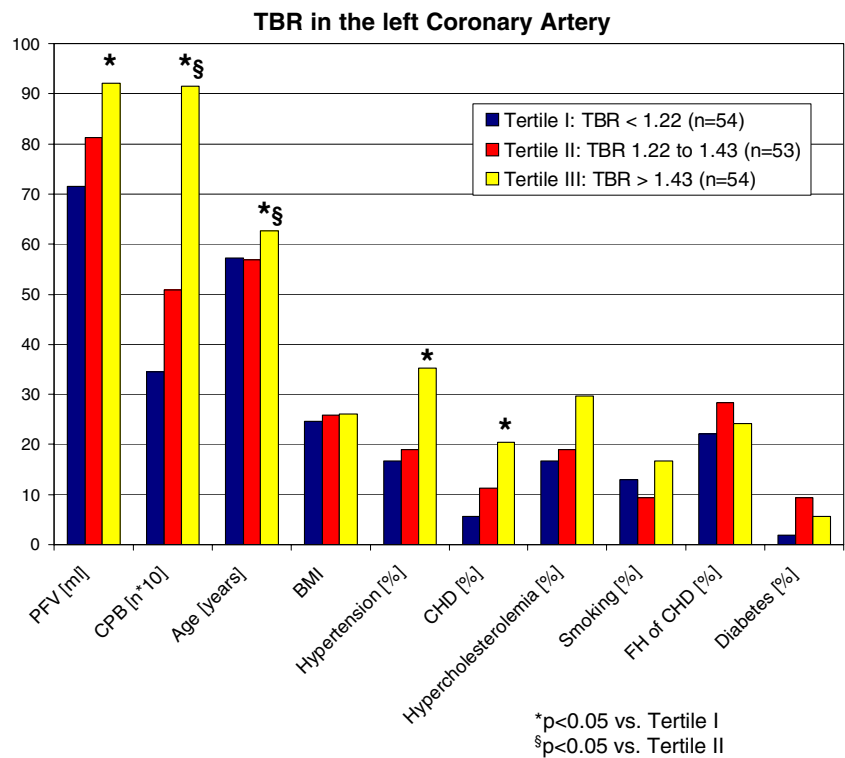
Given these promising results with relatively low performance CT, in seems likely that faster 64- or 128-slice PET/CT scanners, with ECG-triggered CT acquisition, will reliably assign FDG uptake to the major coronary arteries. This innovation should permit TBR measurements in the entire coronary tree, and furthermore allow the identification and characterization of specific coronary lesions such as calcified or non-calcified plaques [15].

We were able to obtain TBR measurements in the one half of our study population in whom myocardial FDG uptake was low. The absence of demographic or risk factor differences between patients with and without myocardial uptake suggests that our findings could be generalized to the population as a whole. However, obtaining more

reliable suppression of myocardial FDG uptake is a precondition for general application of FDG PET/CT in future clinical trials, especially given that the myocardial metabolic pattern can vary in different regions at the same time as well as at different times in the same region [25]. For precisely this reason, patients in the study by Wykrzykowska et al. [24] were offered a low-carbohydrate, high-fat meal the night before the PET/CT scan and were asked to drink a vegetable oil beverage the morning of the study. In spite of these efforts to suppress myocardial FDG uptake, adequate suppression was obtained in only 20 of 32 patients (63%), a proportion only slightly higher than that seen in our study (55%) without any special patient preparation. Therefore, there
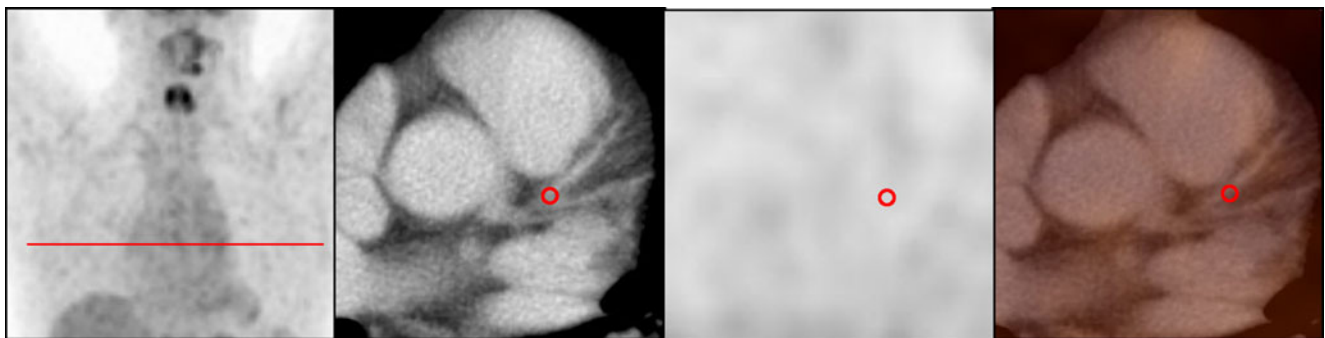

Fig. 4 PET/CT images of a 75-year-old female patient with no coronary risk factors. Coronal PET image shows no myocardial FDG uptake. *Red circle* indicates ROI. Axial CT images enable the exact anatomical localization of the left coronary artery. The SUV_{max} in the left coronary artery was 0.8, the mean venous SUV was 1.1 and the maximum TBR_{LAD} was 0.74 (low tertile). PFV was 65.3 ml
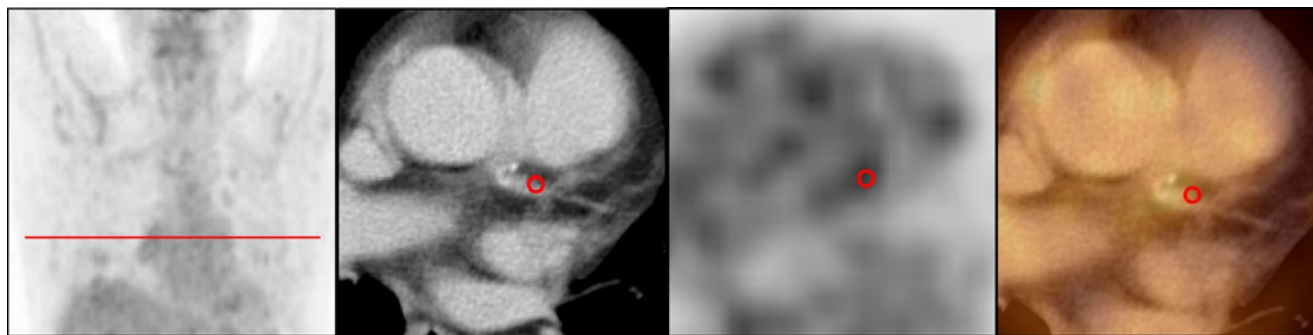
Fig. 5 PET/CT images of a 66-year-old male patient with coronary heart disease, a history of hypertension and smoking. *Red circle* indicates ROI. Coronal PET image shows no myocardial FDG uptake. Axial CT images allow identification of the anatomical location of the left coronary artery. The SUV_{max} in the left coronary artery was 1.6 and mean venous SUV was 1.1, resulting into a maximum TBR_{LAD} of 1.45 (high tertile). The PFV was 175.9 ml

remains a need to develop superior dietary or fasting protocols for future FDG PET/CT investigations of the coronary arteries.

Combined PET/CT offers the additional opportunity to image several markers for atherosclerosis from the same scanning session. In the present study, estimates of calcified atherosclerotic plaque burden and PFV were obtained in addition to the FDG uptake in the coronary arteries. These markers were reliably quantified by PET/CT with excellent intra- and inter-reader reproducibility, in accordance with a previous study by Rudd et al. [26]. Also as previously documented in studies focussing on coronary [16] and peripheral vascular calcifications [27], we found that the magnitude of CPB correlated with all cardiovascular risk factors considered in the present study, save only hypercholesterolaemia. When multiple regression analysis was performed to accommodate for differences in age, BMI and risk factors, correlations between CPB and age, TBR, smoking, diabetes and coronary heart disease remained significant, thus strengthening the inherent association of CP with the presence of atherosclerosis.

Several recent studies have suggested that PFV might also be useful as an independent risk factor for the occurrence of coronary atherosclerosis [17, 18]. Consistent with this claim, we also found PFV to correlate with all of the cardiovascular risk factors except smoking and coronary heart disease. When multiple regression analysis was performed to accommodate for differences in age, BMI and risk factors, correlations between PFV and BMI, age, smoking and CPB remained significant, thus supporting the utility of PFV as an imaging marker for atherosclerotic disease. Our findings are also consistent with a recent study showing an association between PFV and the number of atherosclerotic plaques in the coronary arteries [18]. Consistent with another previous report [28], our PFV findings showed a significant correlation with the amount of vascular calcification, as assessed by the CPB score.

Together, these findings call for exploiting the several morphological and functional imaging markers obtainable by FDG PET/CT, so as to define a combination of variables most sensitively predictive of future cardiovascular events, with general applicability extending beyond the setting of clinical oncology.

Limitations

As noted above, myocardial FDG uptake hampered to a variable extent the analysis of FDG uptake in the LAD (see Fig. 1b). We necessarily excluded from further consideration the patients with discernible myocardial FDG uptake, who constituted almost one half of the original study group. The excluded patient group, however, showed no significant differences in their cardiovascular risk profile, so that this should not have led to a major selection bias influencing the main conclusions of the study. This study was performed in tumour patients, and consequently its findings might not be generalized to other patient populations. However, the stringent national guidelines for recruitment of healthy control subjects (related to radiation exposure) necessitated the present use of an ill cohort. Due to the requirements of oncological investigation, the acquisition of the PET/CT images was started approximately 60 min after FDG injection. An acquisition beginning at 90 or 120 min post-injection might be superior for evaluation of arterial FDG uptake [26], although others have noted stable TBR values in aortic plaques during 3 h after FDG injection [29]. Furthermore, given the known susceptibility of the right coronary artery to motion artefacts, especially in the absence of ECG gating, with consequent blurring of both the CT and PET images and given that only non-cardiac scans were available in the present retrospective study, it was not possible to display the complete coronary tree in all patients. Therefore, we of necessity used a standardized evaluation targeting only the

proximal portion of the LAD. Despite these caveats, the findings of our study were still significant, and we speculate that more compelling results with higher correlation coefficients would have emerged had we used a protocol optimized for vascular imaging.

Conclusion

The findings of this cross-sectional study show that FDG uptake in the LAD correlates with conventional cardiovascular risk factors, such as hypertension, coronary heart disease and BMI, and with imaging-based markers of atherosclerosis, such as PFV and CPB. FDG uptake quantifications of the coronary arteries might be useful in order to detect the local inflammatory activity of coronary artery lesions and ultimately to help identify patients at risk for future cardiovascular events. However, current methods prevent the general use of this procedure due to imperfect suppression of myocardial FDG uptake.

References

1. Lloyd-Jones D, Adams R, Carnethon M, De Simone G, Ferguson TB, Flegal K, et al. Heart disease and stroke statistics–2009 update: a report from the American Heart Association Statistics Committee and Stroke Statistics Subcommittee. Circulation 2009;119:e21–181. doi:CIRCULATIONAHA.108.191261 [pii] 10.1161/CIRCULATIONAHA.108.191261.
2. Naghavi M, Libby P, Falk E, Casscells SW, Litovsky S, Rumberger J, et al. From vulnerable plaque to vulnerable patient: a call for new definitions and risk assessment strategies: Part II. Circulation 2003;108:1772–8. doi:10.1161/01.CIR.0000087481.55887.C9 108/15/1772 [pii].
3. Naghavi M, Libby P, Falk E, Casscells SW, Litovsky S, Rumberger J, et al. From vulnerable plaque to vulnerable patient: a call for new definitions and risk assessment strategies: Part I. Circulation 2003;108:1664–72. doi:10.1161/01.CIR.0000087480.94275.97 108/14/1664 [pii].
4. Hansson GK. Inflammation, atherosclerosis, and coronary artery disease. N Engl J Med 2005;352:1685–95. doi:352/16/1685 [pii] 10.1056/NEJMra043430.
5. Saam T, Hatsukami TS, Takaya N, Chu B, Underhill H, Kerwin WS, et al. The vulnerable, or high-risk, atherosclerotic plaque: noninvasive MR imaging for characterization and assessment. Radiology 2007;244:64–77. doi:244/1/64 [pii] 10.1148/radiol.2441051769.
6. Rudd JH, Myers KS, Bansilal S, Machac J, Rafique A, Farkouh M, et al. (18)Fluorodeoxyglucose positron emission tomography imaging of atherosclerotic plaque inflammation is highly reproducible: implications for atherosclerosis therapy trials. J Am Coll Cardiol 2007;50:892–6. doi:S0735-1097(07)01825-6 [pii] 10.1016/j.jacc.2007.05.024.
7. Rudd JH, Warburton EA, Fryer TD, Jones HA, Clark JC, Antoun N, et al. Imaging atherosclerotic plaque inflammation with [18F]-fluorodeoxyglucose positron emission tomography. Circulation 2002;105:2708–11.
8. Tawakol A, Migrino RQ, Bashian GG, Bedri S, Vermylen D, Cury RC, et al. In vivo 18F-fluorodeoxyglucose positron emission tomography imaging provides a noninvasive measure of carotid plaque inflammation in patients. J Am Coll Cardiol 2006;48:1818–24. doi:S0735-1097(06)01980-2 [pii] 10.1016/j.jacc.2006.05.076.
9. Ben-Haim S, Kupzov E, Tamir A, Israel O. Evaluation of 18F-FDG uptake and arterial wall calcifications using 18F-FDG PET/CT. J Nucl Med 2004;45:1816–21. doi:45/11/1816 [pii].
10. Bural GG, Torigian DA, Chamroonrat W, Houseni M, Chen W, Basu S, et al. FDG-PET is an effective imaging modality to detect and quantify age-related atherosclerosis in large arteries. Eur J Nucl Med Mol Imaging 2008;35:562–9. doi:10.1007/s00259-007-0528-9.
11. Rominger A, Saam T, Wolpers S, Cyran CC, Schmidt M, Foerster S, et al. 18F-FDG PET/CT identifies patients at risk for future vascular events in an otherwise asymptomatic cohort with neoplastic disease. J Nucl Med 2009;50:1611–20. doi:jnumed.109.065151 [pii] 10.2967/jnumed.109.065151.
12. Virmani R, Burke AP, Farb A, Kolodgie FD. Pathology of the vulnerable plaque. J Am Coll Cardiol 2006;47:C13–8. doi:S0735-1097(05)03137-2 [pii] 10.1016/j.jacc.2005.10.065.
13. Ambrose JA, Tannenbaum MA, Alexopoulos D, Hjemdahl-Monsen CE, Leavy J, Weiss M, et al. Angiographic progression of coronary artery disease and the development of myocardial infarction. J Am Coll Cardiol 1988;12:56–62. doi:0735-1097(88)90356-7 [pii].
14. Nissen SE. IVUS is redefining atherosclerotic disease. Am J Manag Care 2003;Suppl:2–3. doi:3356 [pii].
15. Leber AW, Becker A, Knez A, von Ziegler F, Sirol M, Nikolaou K, et al. Accuracy of 64-slice computed tomography to classify and quantify plaque volumes in the proximal coronary system: a comparative study using intravascular ultrasound. J Am Coll Cardiol 2006;47:672–7. doi:S0735-1097(05)03035-4 [pii] 10.1016/j.jacc.2005.10.058.
16. Budoff MJ, Shaw LJ, Liu ST, Weinstein SR, Mosler TP, Tseng PH, et al. Long-term prognosis associated with coronary calcification: observations from a registry of 25,253 patients. J Am Coll Cardiol 2007;49:1860–70. doi:S0735-1097(07)00680-8 [pii] 10.1016/j.jacc.2006.10.079.
17. Ding J, Hsu FC, Harris TB, Liu Y, Kritchevsky SB, Szklo M, et al. The association of pericardial fat with incident coronary heart disease: the Multi-Ethnic Study of Atherosclerosis (MESA). Am J Clin Nutr 2009;90:499–504. doi:ajcn.2008.27358 [pii] 10.3945/ajcn.2008.27358.
18. Greif M, Becker A, von Ziegler F, Lebherz C, Lehrke M, Broedl UC, et al. Pericardial adipose tissue determined by dual source CT is a risk factor for coronary atherosclerosis. Arterioscler Thromb Vasc Biol 2009;29:781–6. doi:ATVBAHA.108.180653 [pii] 10.1161/ATVBAHA.108.180653.
19. Rominger A, Saam T, Vogl E, Übleis C, la Fougère C, Foerster S, et al. In-vivo imaging of macrophage activity in the coronary arteries using 68 Ga-DOTA-TATE PET/CT: correlation with coronary calcium burden and risk factors. J Nucl Med 2010;51:193–7. doi:jnumed.109.070672 [pii] 10.2967/jnumed.109.070672
20. Nichols JH, Samy B, Nasir K, Fox CS, Schulze PC, Bamberg F, et al. Volumetric measurement of pericardial adipose tissue from contrast-enhanced coronary computed tomography angiography: a reproducibility study. J Cardiovasc Comput Tomogr 2008;2:288–95. doi:S1934-5925(08)00559-5 [pii] 10.1016/j.jcct.2008.08.008.
21. Bland JM, Altman DG. Statistical methods for assessing agreement between two methods of clinical measurement. Lancet 1986;1:307–10.

22. Paulmier B, Duet M, Khayat R, Pierquet-Ghazzar N, Laissy JP, Maunoury C, et al. Arterial wall uptake of fluorodeoxyglucose on PET imaging in stable cancer disease patients indicates higher risk for cardiovascular events. J Nucl Cardiol 2008;15:209–17. doi: S1071-3581(08)00028-7 [pii] 10.1016/j.nuclcard.2007.10.009.

23. Yun M, Jang S, Cucchiara A, Newberg AB, Alavi A. 18F FDG uptake in the large arteries: a correlation study with the atherogenic risk factors. Semin Nucl Med 2002;32:70–6. doi: S0001299802500076 [pii].

24. Wykrzykowska J, Lehman S, Williams G, Parker JA, Palmer MR, Varkey S, et al. Imaging of inflamed and vulnerable plaque in coronary arteries with 18F-FDG PET/CT in patients with suppression of myocardial uptake using a low-carbohydrate, high-fat preparation. J Nucl Med 2009;50:563–8. doi: jnumed.108.055616 [pii] 10.2967/jnumed.108.055616.

25. Inglese E, Leva L, Matheoud R, Sacchetti G, Secco C, Gandolfo P, et al. Spatial and temporal heterogeneity of regional myocardial uptake in patients without heart disease under fasting conditions on repeated whole-body 18F-FDG PET/CT. J Nucl Med 2007;48:1662–9. doi:jnumed.107.041574 [pii] 10.2967/jnumed.107.041574.

26. Rudd JH, Myers KS, Bansilal S, Machac J, Pinto CA, Tong C, et al. Atherosclerosis inflammation imaging with 18F-FDG PET: carotid, iliac, and femoral uptake reproducibility, quantification methods, and recommendations. J Nucl Med 2008;49:871–8. doi: jnumed.107.050294 [pii] 10.2967/jnumed.107.050294.

27. Eisen A, Tenenbaum A, Koren-Morag N, Tanne D, Shemesh J, Imazio M, et al. Calcification of the thoracic aorta as detected by spiral computed tomography among stable angina pectoris patients: association with cardiovascular events and death. Circulation 2008;118:1328–34. doi:CIRCULATIONAHA.107.712141 [pii] 10.1161/CIRCULATIONAHA.107.712141.

28. Rosito GA, Massaro JM, Hoffmann U, Ruberg FL, Mahabadi AA, Vasan RS, et al. Pericardial fat, visceral abdominal fat, cardiovascular disease risk factors, and vascular calcification in a community-based sample: the Framingham Heart Study. Circulation 2008;117:605–13. doi:CIRCULATIONAHA.107.743062 [pii] 10.1161/CIRCULATIONAHA.107.743062.

29. Menezes LJ, Kotze CW, Hutton BF, Endozo R, Dickson JC, Cullum I, et al. Vascular inflammation imaging with 18F-FDG PET/CT: when to image? J Nucl Med 2009;50:854–7. doi: jnumed.108.061432 [pii] 10.2967/jnumed.108.061432.